IEEE Access
Multidisciplinary | Rapid Review | Open Access Journal

Received 3 March 2023, accepted 31 March 2023, date of publication 24 April 2023, date of current version 27 April 2023.

Digital Object Identifier 10.1109/ACCESS.2023.3269423

RESEARCH ARTICLE

Multi-Period Hybrid AC/DC-OPF Model for Flexibility Market Clearing With Seamless TSO-DSO Coordination

DAMIAN SIERASZEWSKI[1], OLE KJÆRLAND OLSEN[1], DMYTRO IVANKO[1,2], IRINA OLEINIKOVA[1], AND HOSSEIN FARAHMAND[1], (Senior Member, IEEE)

[1]Department of Electric Power Engineering, Norwegian University of Science and Technology, 7034 Trondheim, Norway
[2]NORCE Norwegian Research Centre, 4021 Stavanger, Norway

Corresponding author: Dmytro Ivanko (dmytro.ivanko@ntnu.no)

This work was supported in part by the ERA-Net Project HONOR (RegSys 2018) under Grant 646039 and Grant 7759750, and in part by the Framework of the Joint Programming Initiative ERA-Net Smart Energy Systems funded by the European Union's Horizon 2020 Research and Innovation Program.

ABSTRACT Unlocking flexibility assets from the consumer side and developing a well-functioning flexibility market (FM) is crucial to address the oncoming challenges in the EU power grid. In these conditions, the coordination between distribution system operators (DSOs) and transmission system operators (TSOs) remains a critical task for optimally harvesting flexibility services. For that reason, this paper focuses on investigating the instruments for FM market design and modelling, which ensures proper TSO-DSO coordination. First, the paper introduces the scheme and strategy for FM operation and coordination in Norwegian conditions. After, the multi-period hybrid AC/DC-OPF model for FM modelling is presented. This model combines optimal power flow (OPF) methods consisting of a second-order cone (SOC)-ACOPF, which is applied for the distribution grid and DC-OPF for the transmission grid. The model was validated and tested based on grid configurations from existing projects, where it showed high accuracy and applicability. Finally, an example of solving grid challenges in a distribution grid with the help of flexibility services was presented. The outcomes of this paper propose valuable tools for establishing an effective flexibility exchange mechanism between TSO and DSO.

INDEX TERMS TSO-DSO interaction, power flow modeling, flexibility market, distributed energy resources, distributed flexibility assets.

I. NOMENCLATURE

Indices and Sets

N/n	Sets/index of nodes in DCOPF model.
M/m	Sets/index of nodes in SOC-ACOPF model.
T/t	Sets/index of hours for the model.
U/u	Sets/index of time units for the model.
j	Index of receiving node, for both DCOPF and SOC-ACOPF.

Parameters

B_{nj}	B-matrix for DCOPF model.
G_{mj}	G-matrix for SOC-ACOPF model.
B_{mj}	B-matrix for SOC-ACOPF model.
$P^{L,AC}$	Active load in SOC-ACOPF model.
$Q^{L,AC}$	Reactive load in SOC-ACOPF model.
$P^{G,AC,max}$	Maximum active power production in SOC-ACOPF.
$P^{G,AC,min}$	Minimum active power production in SOC-ACOPF.
$Q^{G,AC,max}$	Maximum reactive power production in SOC-ACOPF.
$Q^{G,AC,min}$	Minimum reactive power production in SOC-ACOPF.
$P^{L,DC}$	Active load in DCOPF model.
$P^{G,DC,max}$	Maximum active power production in DCOPF.

The associate editor coordinating the review of this manuscript and approving it for publication was Siqi Bu.

$P^{G,DC,min}$	Minimum active power production in DCOPF.
$P^{fl,max}$	Maximum active power flow in DCOPF.
θ^{slack}	Voltage angle for slack bus in DCOPF.
$P^{G,Flex,max}$	Maximum flexible active power production.
$P^{G,Flex,min}$	Minimum flexible active power production.
$P^{L,Flex,max}$	Maximum flexible load.
$P^{L,Flex,min}$	Minimum flexible load.
$P^{SoC,init}$	Initial state of charge of the battery.
$P^{SoC,max}$	Maximum state of charge of the battery.
$P^{SoC,min}$	Minimum state of charge of the battery.
$P^{ch,max}$	Maximum charging of the battery.
$P^{disch,max}$	Maximum discharging of the battery.
η^{ch}	Charging efficiency of the battery.
η^{disch}	Discharging efficiency of the battery.
c^{G}	Production price.
c^{Flex}	Flexible price.
c^{Batt}	Battery price.
c^{LS}	Load Shedding price.

Variables

u_m	Auxiliary variable for: $\frac{V_m^2}{\sqrt{2}}$.
R_{mj}	Auxiliary variable for: $V_m V_j cos(\theta)$.
I_{mj}	Auxiliary variable for: $V_m V_j sin(\theta_{mj})$.
$P^{G,AC}$	Active power production in SOC-ACOPF.
$Q^{G,AC}$	Reactive power production in SOC-ACOPF.
$P^{G,DC}$	Active power production in DCOPF.
P^{fl}	Active power flow in DCOPF.
θ	Voltage angle in DCOPF.
$P^{G,Flex}$	Active flexible power production.
$P^{L,Flex}$	Active flexible load.
P^{LS}	Load shedding.
P^{SoC}	State of charge of the battery.
P^{ch}	Charging of the battery.
P^{disch}	Discharging of the battery.
δ	Binary variable for battery operation.

II. INTRODUCTION

In recent years, the functioning of the European Union (EU) energy systems has been characterized by the growing electrification of society, the introduction of renewable and distributed energy resources (DERs), the widespread use of electric vehicles, and the transition from gas to electric heating in buildings [1]. On the positive side, such energy production and consumption transition lead to a more efficient, sustainable, and low-carbon society. However, at the same time, the rapid increase of these technologies poses significant issues to transmission and distribution grids. Solving the problems with congestion, frequency and voltage control, balancing, and ensuring stable and safe power grid operation are becoming more challenging and crucial tasks than ever before.

The utilization of flexibility assets from the consumer side is a key tool in resolving oncoming challenges in the EU power grid. Such flexibility assets may include Demand Response (DR), Energy Storage System (ESS), Electric Vehicle (EV) charging load, load shifting, and load shedding instruments etc. In order to reveal flexibility potential from energy consumers and prosumers, the development of novel market mechanisms for flexibility planning and procurement is required [2]. In this marketplace, the new actor, called the aggregator, will be responsible for combining flexibility assets from multiple small-scale energy users, allowing them to be involved in FM [3]. The Distribution System Operators (DSOs) and Transmission System Operators (TSOs) will be the main flexibility buyers and most prominent beneficiaries of establishing the new Flexibility Market (FM).

Coordination between TSOs and DSOs is critical for deploying flexibility services. A lack of coordination between the TSOs and DSOs may decrease profit from flexibility resources and have a negative effect on grid performance. In this environment, the roles and responsibilities of participants in the FM are identified in such a way that DSOs and TSOs can support each other efficiently, provide cost-effective operation of the grid, and properly utilise flexibility resources.

The concepts and solutions for TSOs and DSOs coordination in the flexibility marketplace are still under development [4], [5], [6]. The literature demonstrated several possible schemes for TSO-DSO coordination [7], [8], [9]. The SmartNet project has summarized and suggested five possible schemes for FM market operation and coordination, which include centralized FM, local FM, shared balancing responsibility FM, common TSO-DSO FM, and integrated FM [10]. Roles and responsibilities between market participants and overall coordination depend on the chosen market schemes [11]. The feasibility of a particular coordination scheme is affected by the current organization and cooperation of national TSOs and DSOs on one side and the local initiatives to integrate ancillary services markets on the other side. Therefore, it might be required to consider the different schemes and select the best one for TSO-DSO coordination, taking into account the national regulatory framework and local conditions. In view of the Norwegian state of affairs, the local FM coordination scheme was selected as a starting point in our research.

Some publications propose to perform coordination between TSO and DSO based on the Feasible Operating Region (FOR), which represents the aggregated flexibility potential of a distribution grid, by outlining the feasible active and reactive power flows at the TSO-DSO interconnection [34]. The DSO can share the FOR with the TSO to manage the operational issues of the transmission grid.

The paper [36] proposes a linear OPF-based methodology to provide aggregated information on flexibility at the TSO-DSO interconnection point. This model aims to consider flexibility using time series, while the aggregation process is repeated for several time steps, which is essential for short-term operation planning of power systems.

The investigation [35] presents a nodal operating envelope (NOE) modeling framework to assess various DER flexibility features while also accounting for reactive power and network constraints.

The publication [34] provides an in-depth comparison of three different categories of methods for the identification of FOR, which include Geometric methods, Random Sampling (RS) methods, and Optimization-based (OB) methods. The comparison of methods showed that each of them has certain advantages and disadvantages, and methods for better estimation of FOR are still of great interest to researchers worldwide [34].

Implementing reliable and accurate modelling approaches is essential for the proper function of FM. In this concern, the optimal power flow (OPF) is a powerful approach for modelling and optimizing flexibility usage for both economic and technical purposes. Traditionally, the OPF is used to find the optimal settings of a given power grid that optimize a specific objective function while satisfying its power flow equations, system security, equipment operating limits, and other system constraints [12].

There are several approaches for formulation and solving the OPF problem, including AC-OPF, DC-OPF, DistFlow, Linearized DistFlow, a semidefinite programming (SDP) convex relaxation of the model, and a second-order cone programming (SOCP). The in-depth overviews of the OPF modelling techniques with their mathematical formulation are presented [12]. Currently, a number of researchers are investigating the application of OPF algorithms for power market design and modelling. For example, the paper [13] compares commonly used OPF formulations based on the IEEE 33-bus test radial distribution system. The publication shows that several methods and algorithms can be applied for power flow calculation, each having its unique properties, certain advantages, and disadvantages. When deciding upon which OPF technique to use, it is vital to have these different properties in mind depending on the system's characteristics one wants to solve [13]. It should be mentioned that most of the existing publications consider OPF modelling in transmission and distribution grids separately [14]. At the same time, the TSO-DSO coordination in FM based on OPF still requires additional investigation.

III. CONCEPT OF MULTI-PERIOD HYBRID AC/DC-OPF MODEL

In our study, performing power flow analysis and coordination for both the distribution and transmission grid is of interest. Between the two networks, the requirements for the distribution grid are most complex when considering production in sub-branches. A common feature in distribution grids in Norway is the radial structure, where power provision occurs from a single substation and is transferred down several branches and sub-branches to loads (consumers).

Distribution grids have certain difficulties that complicate power flow modellings, such as high R/X ratio, significant number of unbalanced loads, and integration of distributed generation (DG) in sub-branches [15], [16]. These factors may contribute to the radial system being ill-conditioned and raise the convergence problem for AC-OPF [16]. One of the methods that can handle this issue is the Backward-Forward sweep method, which is commonly utilized when performing power flow analysis. However, this method has poor capability in handling active distribution grids and multi-period AC-OPF [16]. Thus, this method is not applicable in our case due to the need to include flexibility assets down in the distribution grid's sub-branches. Therefore, the application of convex approximation methods is required.

Since a TSO-DSO system can be too computationally heavy to solve, the DC Power Flow (DC-OPF) approximation method can simplify the task. DC-OPF is a non-iterative, linearization of the AC-OPF method where specific assumptions are made to ease the computational effort. Some of these assumptions are neglect resistance leading to no power losses and neglecting reactive power in the system [18]. However, DC-OPF is only suitable for transmission grids due to the distribution grid's high R/X ratio. This method is not accurate enough for an active distribution grid. For this reason, DC-OPF can be applied for transmission grid modelling, and another approach should be used for the distribution grid.

Instead of using approximation like the DC-OPF method, the relaxation method of the AC-OPF shows its applicability to the distribution grid. The relaxation extends the feasibility area of the AC-OPF and gives a better convergence area for the distribution grid than the DC-OPF [19]. The general benefits for the convex relaxation methods are that they are fast and stable, have better accuracy than the DC-OPF, and always provide a lower or upper bound, which assures global optimum or minimum for the objective function [20]. In order to satisfy the needs of the active distribution grid, the choice fell on the convex relaxation method based on second-order cone programming. The Second-Order Cone AC Optimal Power Flow (SOC-ACOPF) method has reasonably good accuracy and does not require extensive computational power.

Thus, our investigation proposed the multi-period hybrid AC/DC-OPF model, which combines SOC-ACOPF for distribution and DC-OPF for the transmission grid. The model was developed in such a way that seamless coordination between TSOs and DSOs can be achieved. A connection constraint was formulated to combine SOC-ACOPF and DC-OPF models, which defines the distribution grid as a load for the transmission grid. Therefore, any changes occurring in one grid will affect the performance of other grids. The model was then further extended by formulating the power balance equation to include flexibility assets in the distribution grid and criteria for how the flexibility should be activated. Moreover, the model was modified to perform optimization for extended periods in a single simulation to perform multi-period simulations. This paper presents extended results from [23] and [33].

The paper has the following structure. Chapter 3 introduces the selected strategy for FM operation and coordination. Chapter 4 presents the mathematical formulation of the

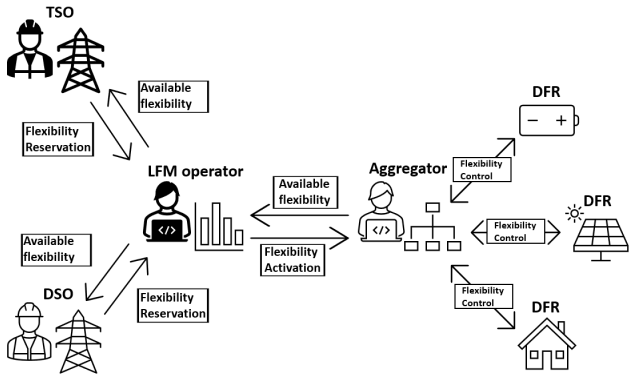

FIGURE 1. Coordination between different market participants in the flexibility market.

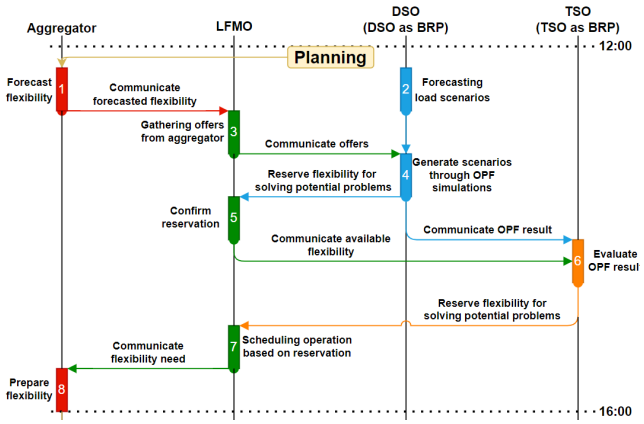

FIGURE 2. Flowchart showing the planning phase in the LFM.

multi-period hybrid AC/DC-OPF model. Chapter 5 demonstrates the testing of the hybrid OPF model and solving challenges in the distribution grid with the utilization of flexibility assets. Finally, the main conclusions of the study are emphasized in Chapter 6.

IV. FM OPERATION AND COORDINATION

This chapter consists of three sections. Each section presents the particular aspects of FM operation and coordination. Section 2.1 considers the coordination between market participants. Section 2.2 introduces the planning and operation phases in the FM platform. Finally, Section 2.3 discusses the application of the OPF model for flexibility procurement.

A. THE MARKET COORDINATION SCHEME

Out of several possible market coordination schemes, the local flexibility market (LFM) design has appeared to be the most fitting for the conditions and tasks of our investigation. LFM can be characterized as an electricity trading platform to provide flexibility in geographically limited areas, such as neighbourhoods, communities, towns, and small cities, which is relevant for Norwegian society [17].

Fig. 1 shows the coordination between different market participants in the proposed LFM platform. In this LFM, TSO and DSO will operate as balancing responsible parties by purchasing flexibility to solve grid problems [21]. The grid problems include uncertain load variations, power shortages, grid congestion, or voltage problems. DSO will prioritise reserving distributed flexibility resources (DFR) to solve potential grid constraints or load variation. The remaining flexibility not needed by the DSO will be available for the TSO to use, as long as the DFR activation respects DSO's grid constraints. The reservation of flexibility assets will be made through an LFM established and controlled by a local market operator according to [10]. In coordinating transmission and distribution systems, we establish a position for the participation of an aggregator who represents decentralized resources in the form of DFR from the end consumer or prosumer side. In more detail, information about coordination between the market participants is given in [22].

The concept of LFM and ways for its coordination is an ongoing field of development, and therefore adjustments for Norwegian conditions are required [24]. If using the Nord Pool Nordic market [25] as a reference, the timeframe for when this market is to operate is between the intraday and balancing markets. After day-ahead market clearing, the planning process will commence, determining the operation for the coming day. This operation is split into quarter-hour time slots, and the whole process will last for 24 hours.

B. PLANNING AND THE OPERATION PHASES IN THE LFM PLATFORM

The LFM strategy can be divided into two phases: the planning phase and the operation phase. The planning phase attempts to proactively find possible grid problems that are perceived to occur before physical operation and a potential solution based on forecasted DFR availability. The operation phase will consist of real-time DFR activation for different periods, evaluating the system's conditions based on the new data, and procuring additional flexibility. Fig. 2 showcases the whole planning phase in the LFM platform. The entire phase starts after the day-ahead market is cleared. Aggregators then identify available DFR capacity for the coming operation and provide offers to the LFMO, which will forward this information to the DSO. In the planning stage, aggregators perform flexibility forecasting, and DSO executes forecasting of load scenarios. These scenarios are then used as input for the OPF simulation, determining potential grid issues and the necessary flexibility to alleviate them. DSO can then decide the right course of action to either reserve this capacity or wait to see how the situation unfolds. Any desire to reserve flexibility will then be communicated back to the LFMO. TSO will receive both the OPF result from DSO and the information regarding the remaining flexibility. Based on this data, TSO can evaluate reserving flexibility for their use.

According to the flexibility reservation from DSO and TSO, LFMO will construct an operation schedule for the coming day. This schedule will be provided to the aggregators, informing them of their respective flexibility dispatch [33].

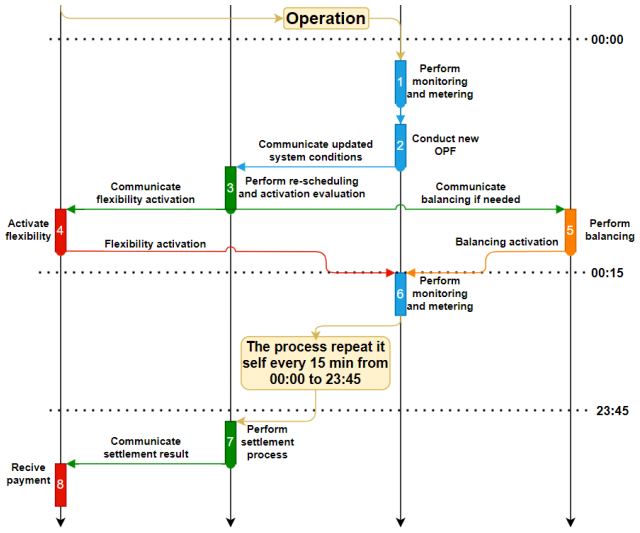

FIGURE 3. Flowchart showing the operation phase in the LFM.

After the completion of the planning phase, the operation phase will commence, as shown in Fig 3. Before activation, DSO will evaluate the grid's situation by performing monitoring and metering. This new information will be provided as input to the OPF to acquire more accurate results for the DFR activation, which will then be communicated to LFMO. This is where the strategy of rolling horizon comes into play by re-scheduling the operation based on the most updated information to execute a more accurate and updated DFR activation [33]. Information regarding DFR activation will then be forwarded to aggregators, which will result in the flexibility provision. In the case of insufficient DFR capacity activation, LFMO will communicate this to TSO, who can acquire additional capacity from the wholesale balancing market. While conducting this activation, DSO will again evaluate the grid's situation. The process only applies for one quarter-hour (15 minutes). When the following time frame begins at 00:15, the whole process from 1 to 6 will start over. This procedure repeats for each quarter of the entire day.

After the operation has concluded, the settlement process begins. LFMO will receive information regarding the metering from the BRPs. Based on this information, LFMO will confirm the proper activation of DFR. In the last step, aggregators will receive their required payment from the LFMO accordingly to the provided flexibility [33].

C. APPLICATION OF OPF MODEL FOR FLEXIBILITY PROCUREMENT

In order to effectively determine and activate the necessary flexible capacity, a hybrid multi-period AC/DC-OPF model is deemed preferable for the LFM strategy. This OPF model can be used for creating numerous scenarios representing possible grid situations that may unfold during the coming operation day, including their probability of occurrence [33]. The approach allows the market participants to prepare necessary measures and react to challenges in advance, such as proclaiming or reserving DFR to prevent grid problems that

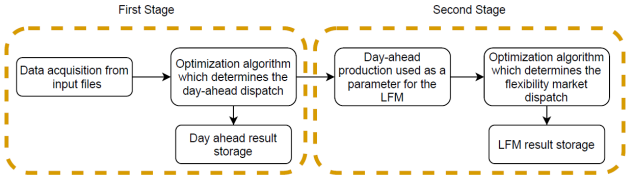

FIGURE 4. Optimization procedure conducted by the multi-period hybrid AC/DC-OPF model.

seem most likely to occur. The development of probabilistic scenarios for FM operation is a complex and important problem. However, since this article is mainly focused on developing AC/DC-OPF model, the issues related to scenarios are not presented in this investigation.

As we can see, the OPF model is an essential part of the FM regarding planning and optimizing flexibility usage for both economic and technical purposes. To achieve this, the optimal power flow simulation needs to meet specific criteria:

- Must be able to solve power flow simulations for transmission and distribution grids with different constraints.
- Need to run power flow for different scenarios for deciding flexibility activation based on the outcome of said scenario.
- Be able to perform multi-period simulations over several time periods.

In our research, it is decided to perform the OPF modelling in two stages [33]. The first optimization simulates the day-ahead market and attempts to find the day-ahead dispatch. The day-ahead generation is then provided to the model as a parameter for the LFM optimization algorithm, where the optimization. The results for both operations are then stored in the files, which enables their further analysis. Fig. 4 presents a flowchart describing the model's operation.

The mathematical formulation of the hybrid multi-period AC/DC-OPF model, which satisfies all mentioned above criteria and tasks, is presented in Chapter 3.

V. MATHEMATICAL FORMULATION OF THE HYBRID AC/DC-OPF MODEL

The main goal of the developed OPF model is to explore how flexibility in the distribution grid can benefit DSO and TSO. Therefore, it is necessary that the OPF model could take into account the impact of resource activation in the distribution grid on the operation of the transmission grid. Therefore, this chapter presents the hybrid OPF model, which combines SOC-ACOPF formulation for the distribution grid and DC-OPF for the transmission grid. Chapter 2 includes two sections. Section 3.1 presents the mathematical formulation of the OPF model, which can be used for the day ahead market clearing. Section 3.2 shows the multi-period hybrid AC/DC-OPF model for trading the flexibility assets between the intraday and balancing markets.

A. FORMULATION OF THE POWER FLOW OPTIMIZATION PROBLEM

As was mentioned before, the OPF problem for TSO-DSO coordination consists of two power flow-solving methods.

For the distribution grid, a SOC-ACOPF (also called Jabr's model) [26] is formulated and further customized [27] to incorporate cost function and production in sub-feeder nodes. For the transmission grid, a DC-OPF is formulated according to [28].

Since the SOC-ACOPF method is more advanced than DC-OPF, some additional information about SOC-ACOPF should be given. The considered SOC-ACOPF method includes three convexified equations with three auxiliary variables u_m, R_{mj}, and I_{mj}, which define the power flow problem. The two power balance equations (1) and (2) state that the flow of power in and out of a given node should be equal to the total amount of production and consumption on the said node.

$$P_m^{L,AC} - P_m^{G,AC} = \sqrt{2}u_m \sum_{j\in k(m)} G_{mj} + \sum_{j\in k(j)} (G_{mj}R_{mj} - B_{mj}I_{mj}) \quad (1)$$

The equation for reactive power balance:

$$Q_m^{L,AC} - Q_m^{G,AC} = -\sqrt{2}u_m \sum_{j\in k(m)} B_{mj} + \sum_{j\in k(m)} (B_{mj}R_{mj} + G_{mj}I_{mj}) \quad (2)$$

The two power balance equations result in two equations with three variables. To be able to solve this system, the third equation (3) is needed. This equation comes in the form of a squared voltage mismatch, which will approach zero as the system converges.

$$2u_m u_j \geq R_{mj}^2 + I_{mj}^2 \quad (3)$$

For both DC-OPF and SOC-ACOPF problems, the same objective function was developed: procuring production to the lowest overall cost while still satisfying grid constraints for both the distribution and transmission grids. Thus, by combining DC-OPF and SOC-ACOPF methods, the hybrid optimization problem can be formulated, as shown in Mathematical Formulation of Hybrid AC/DC-OPF model.

The power production variable and load parameters with the mark "AC" refer to the distribution grid and "DC" to the transmission grid. The combination of all the variables from the SOC-ACOPF and DC-OPF leads to a system with eight variables. These consist of auxiliary variables, active and reactive production, power flow, and voltage angle. The optimization objective will remain the same as for the standalone SOC-ACOPF and DC-OPF methods. The two objectives (4) will be combined to simultaneously minimize operational costs for both the distribution and transmission grid.

One additional constraint introduced into the OPF problem is the AC to DC connection constraint, which connects the distribution grid to the transmission grid. This constraint requires one distribution node to be defined as a feeder/slack node that supplies the power to the grid. While the distribution grid sees this node as a production node, it appears as a single load from the transmission grid's perspective. The criteria for activation of this constraint is that the production for the feeder node ($P_m^{G,AC}$) needs to be equal to the transmission system's load ($P_n^{L,DC}$) if a connection between these nodes is established. This constraint resembles a DC power-balance constrain, where the DC load parameter ($P_n^{L,DC}$) has been replaced by the AC production variable ($P_m^{G,AC}$) in the distribution grid.

Mathematical Formulation of Hybrid AC/DC-OPF model

Variables DC-OPF: $P_n^{G,DC},\ P_{nj}^{fl},\ \theta_n$

Variables SOC-ACOPF: $u_m,\ R_{mj},\ I_{mj},\ P_m^{G,AC},\ Q_m^{G,AC}$

Minimize:

$$\sum_{n=1\ldots N} P_n^{G,DC}\cdot c_n^G + \sum_{m=2\ldots M} P_m^{G,AC}\cdot c_m^G \quad (4)$$

Subject to SOC-ACOPF constraints:

$$(1), \qquad m = 1\ldots M \quad (5a)$$
$$(2), \qquad m = 1\ldots M \quad (5b)$$
$$(3), \qquad \text{for all } mj \quad (5c)$$
$$R_{mj} \geq 0, \qquad \text{for all } mj \quad (5d)$$
$$u_1 = V_1^2/\sqrt{2}, \quad u_m \geq 0, \qquad m = 2\ldots M \quad (5e)$$
$$P_m^{G,AC,min} \leq P_m^{G,AC} \leq P_m^{G,AC,max}, \quad m = 1\ldots M \quad (5f)$$
$$Q_m^{G,AC,min} \leq Q_m^{G,AC} \leq Q_m^{G,AC,max}, \quad m = 1\ldots M \quad (5g)$$

Subject to AC to DC connection constraints:

$$P_n^{G,DC} - P_m^{G,AC} = -\sum_{j\in k(n)} B_{nj}\theta_j, \quad \substack{P_m^{G,AC}=P_n^{L,DC} \\ if \\ n_{DC} = m_{AC}} \quad (6)$$

Subject to DC-OPF constraints:

$$P_n^{G,DC} - P_m^{L,DC} = -\sum_{j\in k(n)} B_{nj}\theta_j, \quad \substack{n=1\ldots N \\ \wedge \\ n_{DC} \neq m_{AC}} \quad (7a)$$
$$P_{nj}^{fl} = B_{nj}(\theta_n - \theta_j), \qquad \text{for all } nj \quad (7b)$$
$$-P_{nj}^{fl,max} \leq P_{nj}^{fl} \leq P_{nj}^{fl,max}, \qquad \text{for all } nj \quad (7c)$$
$$P_n^{G,DC,min} \leq P_n^{G,DC} \leq P_n^{G,DC,max}, \quad n = 1\ldots N \quad (7d)$$
$$\theta_n^{slack} = 0, \quad \substack{\exists!\ n_{DC} \\ \wedge \\ n_{DC} \neq m_{AC}} \quad (7e)$$

Another modification is the reformulated constraint criteria for the power balance equation and slack bus voltage angle. The new criteria for the power balance constraint are that activating this constraint will only happen as long as the transmission node is not connected to a distribution node. Moreover, the slack voltage angle can only be applied to a node not connected to the distribution feeder/slack node.

B. FLEXIBILITY MODELING THROUGH A MULTI-PERIOD POWER FLOW

Efficient optimization of flexibility use requires the system's operation to be determined for an extended period within a single simulation. For this purpose, the hybrid AC/DC-OPF

model has been expanded to include a multi-period optimization approach. The periods within the model are, t and u due to the hourly nature of the day-ahead market and quarterly time units of the flexibility market. This way, the model can find the optimal objective value for a predefined period, which included each variable across every hour and time unit within each hour [33].

Multi-Period Flexibility Optimization Model

Flexibility Variables: $P^{G,Flex}_{m,t,u}$, $P^{L,Flex}_{m,t,u}$, $P^{LS}_{m,t,u}$, $P^{SoC}_{m,t,u}$, $P^{ch}_{m,t,u}$, $P^{disch}_{m,t,u}$

Minimize:

$$\begin{aligned}&\sum_{n=1...N}\sum_{t=1...T}\sum_{u=1...U} P^{G,DC}_{n,t,u}\cdot c^{G}_{n,t,u}\\&+\sum_{m=2...M}\sum_{t=1...T}\sum_{u=1...U}(P^{G,AC}_{m,t,u}\cdot c^{G}_{m,t,u}\\&+(P^{G,Flex}_{m,t,u}-P^{L,Flex}_{m,t,u})\cdot c^{Flex}_{m,t,u}\\&+(P^{disch}_{m,t,u}-P^{ch}_{m,t,u})\cdot c^{batt}_{m,t,u}+P^{LS}_{m,t,u}\cdot c^{LS}_{m,t,u})\end{aligned}\tag{8}$$

Subject to SOC-ACOPF constraints:

$$\begin{aligned}&P^{L,AC}_{m,t,u}+P^{L,Flex}_{m,t,u}-P^{G,AC}_{m,t,u}\\&\quad-P^{G,Flex}_{m,t,u}+P^{ch}_{m,t,u}-P^{disch}_{m,t,u}=\sqrt{2}u_{m,t,u}\\&\sum_{j\in k(m)}G_{mj}+\sum_{j\in k(m)}(G_{mj}R_{mj,t,u}-B_{mj}I_{mj,t,u})\end{aligned}\tag{9}$$

Subject to load shedding constraints:

$$P^{LS}_{m,t,u}=P^{L,AC}_{m,t,u}\tag{10}$$

Subject to flexible generation constraints:

$$P^{G,Flex,min}_{m,t,u}\le P^{G,Flex}_{m,t,u}\le P^{G,Flex,max}_{m,t,u}\tag{11}$$

Subject to flexible load constraints:

$$P^{L,Flex,min}_{m,t,u}\le P^{L,Flex}_{m,t,u}\le P^{L,Flex,max}_{m,t,u}\tag{12a}$$

$$\sum_{m=2...M}\sum_{=1...T}\sum_{u=1...U}P^{L,Flex}_{m,t,u}=0\tag{12b}$$

Subject to battery constraints:

$$P^{SoC,min}_{m,t,u}\le P^{SoC}_{m,t,u}\le P^{SoC,max}_{m,t,u}\tag{13a}$$

$$P^{ch,min}_{m,t,u}\le P^{ch}_{m,t,u}\cdot(1-\delta_{m,t,u})\le P^{ch,max}_{m,t,u}\tag{13b}$$

$$P^{disch,min}_{m,t,u}\le P^{disch}_{m,t,u}\cdot\delta_{m,t,u}\le P^{disch,max}_{m,t,u}\tag{13c}$$

$$P^{SoC}_{m,1,1}=P^{SoC,init}_{m}+P^{ch}_{m,1,1}\cdot\eta^{ch}-\frac{P^{disch}_{m,1,1}}{\eta^{disch}}\tag{13d}$$

$$P^{SoC}_{m,t,u}=P^{SoC}_{m,t,u-1}+P^{ch}_{m,t,u}\cdot\eta^{ch}-\frac{P^{disch}_{m,t,u}}{\eta^{disch}}\tag{13e}$$

$$P^{SoC}_{m,t,1}=P^{SoC}_{m,t-1,U}+P^{ch}_{m,t,1}\cdot\eta^{ch}-\frac{P^{disch}_{m,t,1}}{\eta^{disch}}\tag{13f}$$

$$P^{SoC}_{m,T,U}=P^{SoC,init}_{m}\tag{13g}$$

For (9-13g): $\begin{matrix}m=2...M\\t=1...T\\u=1...U\end{matrix}$

Additional constraints, which define the flexibility assets present in the distribution grid, such as generating units, loads, and batteries have also been added to the model. Equation (1) has been updated to include the contribution from the flexibility sources, as shown by equation (9). The production and load are constraints by their specified minimum and maximum limits. In addition, a constraint is implemented for the load (12b), which ensures that the total amount of load used for flexibility purposes is equal to zero. This constraint implements load shifting capability and secures that the load flexibility is not misused to minimize the costs by minimizing the load. To ensure feasibility of the model, load shedding has also been implemented (10), where the entire load can be shed [33].

The battery is constrained by the minimal and maximum state of charge, charge, and discharge capacity as shown by equations (13a), (13b) and (13c). Equations (13b) and (13c) have also been equipped with an expression that prevents simultaneous charging and discharging of the battery. For each time unit of the model, the state of charge of the battery is calculated for the end of that time unit. This means that the state of charge during the first time unit is equal to the initial state of charge and the amount of capacity that has been charged or discharged during that same time unit (13d). Each consequent time unit is then linked to the previous one (13e). If that unit is the first one of the hour, it is linked to the last one of the previous hour (13f). Lastly, the state of charge of the battery at the end of the simulation, is set to be equal to the initial state of charge of the battery (13g).

The optimization function shown in (4) has been updated to also include flexibility provided from DFR as shown in (8).

With this mathematical formulation, optimal use of flexibility can be determined for each simulation unit and the whole simulation in its entirety. In addition, this hybrid model will determine the OPF in both distribution and transmission grids in one single simulation. In order to validate this model, power flow modelling was performed based on several different test cases. The case of study, which was used to validate and test the model, is presented in Chapter 4.

VI. SIMULATION AND TEST CASES

The developed multi-period hybrid AC/DC-OPF model has been implemented in the Python programming language. In order to formulate the optimization problem, an open-source optimization modelling language called Pyomo has been used [29]. For obtaining a solution in Pyomo, the Gurobi solver was used. The developed optimization problem in Pyomo was generalized for different distribution and transmission grids, regardless of their structure. Therefore, this chapter mainly shows the proof of concept rather than solving one specific real-life case.

The configurations and parameters of the distribution and transmission grids used for the test case are based on publically available and well-tested data from previous projects. A typical radial grid has been chosen for the distribution grid with 33 nodes based on the paper [30]. As designed, the transmission grid will use a meshed grid consisting of 9 nodes [31]. The average R/X ratios for transmission and distribution lines

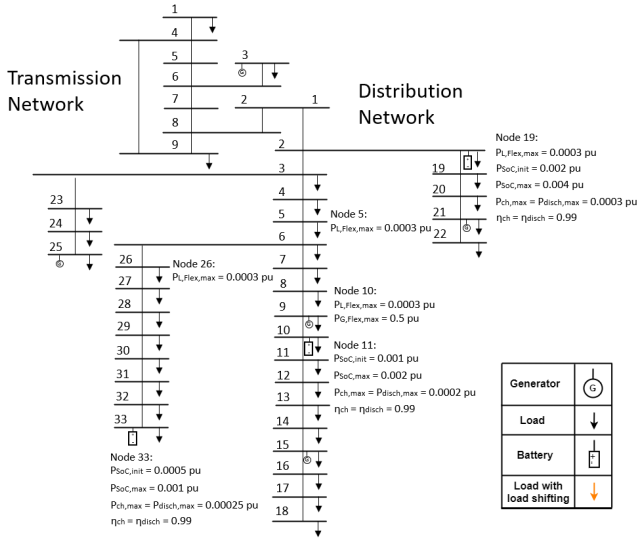

FIGURE 5. Grid configuration for the case of study.

TABLE 1. Basic grid data for distribution and transmission grids.

	Number of nodes	Number of lines	Number of loads	Base voltage [kV]	Base power [MVA]
Distribution grid	33	37	32	12.66	100
Transmission grid	9	9	3	345	100

are 0.11 and 1.44. Detailed information about the parameters of the distribution and transmission grids, including R and X values, are presented in [30] and [31].

Since the TSO-DSO coordination problem in FM is a unique concept, specific customizations have been made to the existing grid models [33]. These changes come in the form of DFR and bidirectional power flow in the grid. The DFR used in this grid include load-shifting, DGs, and batteries. The grid configuration with DFR is shown in Fig 5.

The connection between grids is established by merging two nodes, one from the transmission and the other from the distribution grid. In Fig 5, node two of the transmission and node one of the distribution grids were connected. This way, node one becomes the feeder node for the distribution grid, while transmission's grid node two can be viewed in the distribution grid as a new load. Table 1 presents an overview of the basic data for these two grids.

Additionally, to perform multi-period simulations with varying load profiles and ensure that test cases reflect realistic load scenarios, the data regarding prices and loads from the Nordic power market Nord Pool was taken into account. Table 2 describes the process behind acquiring different DFR prices. For each asset, day ahead price (p_t) has been used as a starting point. This price has then been multiplied with a price factor for each particular type of DFR. This approach allowed determining the price of all DFRs for each time unit while ensuring the relationship between price and demand.

TABLE 2. Price determination for each specific DFR.

	Price for load shifting	Price for flexible generation	Price for charging and discharging of the battery
Day ahead price for a given period	p_t	p_t	p_t
Price factor	0.35	1	0.35
Resulting price for each DFR	$0.35 \cdot p_t$	$1 \cdot p_t$	$0.35 \cdot p_t$

TABLE 3. Result comparison between the combined hybrid AC/DC-OPF model and the standalone DC-OPF and SOC-ACOPF models.

	Active power production [pu]	Reactive power production [pu]	Voltage angle [deg]	Voltage magnitude [pu]
Deviation from DC-OPF	4,87E-05	-	6,30E-04	-
Deviation from SOC-ACOPF	7,00E-05	4,00E-05	1,35E-04	5,49E-05

The chosen approach for generating prices and load data has brought certain simplifications when compared to a real-life scenario. However, the proposed test case is realistic and adequate enough to showcase the multi-period hybrid AC/DC-OPF model as proof of concept.

The validation and testing results for solving challenges in the distribution grid will be presented below in the Sections IV-A-VI-D of this chapter. As can be seen from Table 3, there are some minor deviations between the values produced by these models. The only new concept is the connection constraint. Thus, the comparison demonstrates that the connection between the two methods by setting the feeder node's production equal to the transmission node's load is correct.

A. FLEXIBILITY OPTIMIZATION IN DISTRIBUTION GRID

The use of flexibility assets to optimize the grid operation may result in a more evenly distributed power flow between nodes, reduction of power losses, and voltage drops across the distribution grid. In order to explore how the distribution grid could benefit from flexibility, a case is designed based on optimizing operation with the use of flexibility. The same grid will be simulated in two scenarios, where the flexibility is excluded and included to establish a comparison.

Table 4 shows a comparison of the operation cost in the transmission and distribution grids with and without the use of flexibility assets. As we can see from Table 4, introducing flexibility trading allows us to decrease costs for both transition and distribution systems.

Fig. 6 presents the resulting voltage magnitudes for both cases. The voltage plot in Fig. 6 shows that the case with included flexibility results in a voltage closer to the nominal value of 1 pu, which is the optimal outcome. The most

TABLE 4. Comparing the operation cost of the transmission and distribution grids in a case of flexibility optimization.

Scenario	Distribution grid	Transmission grid
No flexibility	1348.2	123708.5
With flexibility	1327.3	123707.9

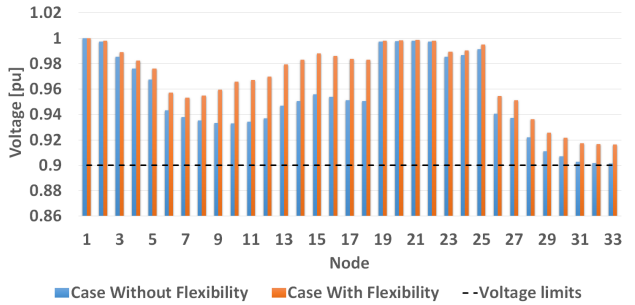

FIGURE 6. The resulting voltage magnitude for all nodes.

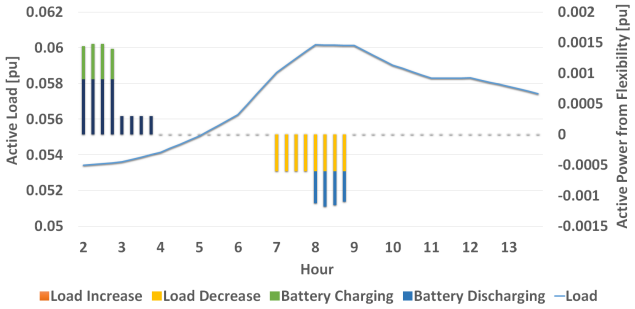

FIGURE 7. Load and battery flexibility is used to optimize the grid.

significant benefits occur between nodes 6 and 18, where the voltage has increased by up to 0.032 pu. Another noticeable improvement is for the nodes 29 to 32, where previously close to minimum bounds voltages are now well above their required limits.

Fig. 7 shows the flexibility used from batteries to optimize the grid operation. From Fig. 7, the flexibility response presents a load increase and charging of batteries during the load's off-peak hours. When the peak hour occurs, an opposite response transpires where the load decreases and batteries are discharged. An important observation is that power production can cover the load since no load shedding has been used.

Fig. 8 analyzes the power injected from transmission to the distribution grid and the resulting change in active power losses. A considerable decrease in the imported active power from the transmission grid has occurred with the inclusion of flexibility in the optimization model, as shown in Fig. 8. This result could be a significant step towards future distribution grid self-sufficiency. A slight decrease in power losses has also occurred due to the reduced current flows within the distribution grid. The result of optimizing distribution operation with flexibility for this case is a decrease of 40 percent in imported active power from the transmission grid and a 7.5 percent decrease in active power losses for the distribution grid [33].

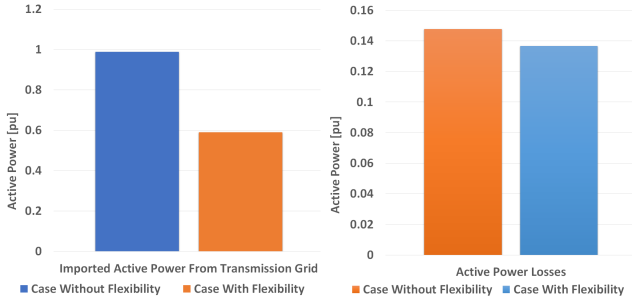

FIGURE 8. Imported active power from the transmission grid and power losses for both cases.

TABLE 5. Comparing the operation cost of the transmission and distribution grids in a case of voltage problems.

Scenario	Distribution grid	Transmission grid
No Flexibility, no voltage regulation	1314	123708.2
With Flexibility, no voltage regulation	1290.7	123708.2
With Flexibility, voltage regulation	1292	123707.7

B. SOLVING VOLTAGE PROBLEMS IN DISTRIBUTION GRID

This test case presents the model's capability to provide voltage regulation. Voltage problems will occur by creating a peak-hour active power consumption in the distribution grid, leading to voltage magnitude below the allowed limits.

According to [32], the minimum criteria are 10 percent above or below nominal voltage value for 10 minutes duration. In our example, the voltage magnitude variation will occur at 08:15. The goal in this test case will focus on solving the voltage magnitude problem in two different ways. One is to restore the voltage magnitude without flexibility, while the second will include it. In order to achieve this voltage regulation, a voltage optimization constraint is implemented in the multi-period hybrid AC/DC-OPF model. This constraint maintains the voltage magnitude within a range of ± 10 percent of the nominal voltage, where the nominal voltage is 1.0 pu. This constraint will force the model to use more of the active power from the DFR to maintain the voltage magnitudes.

Table 5 shows comparison of the operation cost in the transmission and distribution grids in a case of voltage problems. The costs for the distribution grid are increased when voltage regulations are included. It because voltage regulation restricts the feasibility region of the problem by adding additional constraints on the voltage magnitude. Using flexibility assets in the distribution grid allows us to reduce the increase in costs caused by voltage problems.

Fig. 9 presents the voltage magnitude for all nodes.

Fig. 9 shows that voltage profile across all nodes has improved when flexibility assets have been used. To cope with low voltage magnitudes on nodes 28 to 33 due to peak hour consumption, the model has performed different measures for the case with and without flexibility. Without

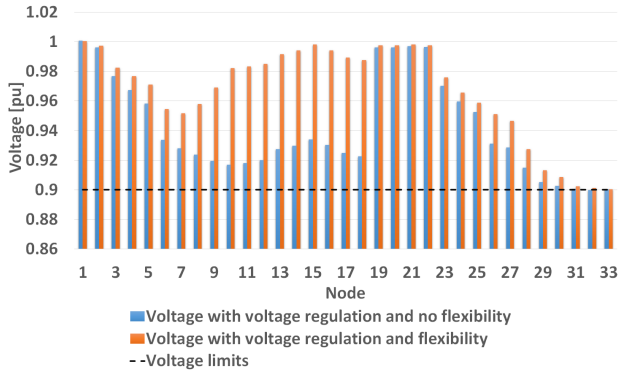

FIGURE 9. Voltage magnitude for all nodes with voltage regulation on node 33.

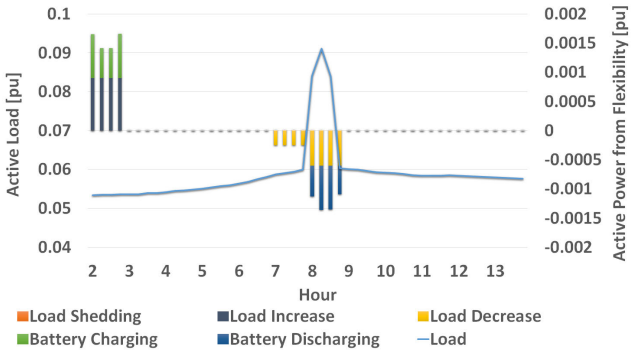

FIGURE 10. The total amount of load-shifting and battery response to the total load in the distribution grid.

flexibility, the optimization model has taken the action of shedding part of the load on nodes 29 to 33 by 0.008 pu, which is not a desirable outcome. This action has led to reduced power injection from the feeder node, resulting in a lower power flow and reduced voltage drop. Such response from the system has made it possible to contain the voltage magnitudes within their allowed limits. For the other case, the capacity provided from flexible assets has allowed maintaining a proper voltage without shedding the load, which is a much more suitable outcome [33].

From Fig. 10, battery charging and load increase occur at the start of the operation. When the peak hour occurs later that day, the battery discharge and load shifting reduce consumption to contain the increased load during that period.

C. SOLVING CONGESTION IN THE DISTRIBUTION GRID

One of the serious problems that can occur in the distribution grid is potential congestion within the grid. When such an unexpected event occurs, the use of flexibility to alleviate this issue can be highly beneficial. Therefore, for this section, a hypothetical lost grid capacity that occurs due to the appearance of an unforeseen event after the day ahead of production has been modelled in the line between nodes 26 and 27.

Three cases have been simulated to answer how the model would respond to the congestion. The first case is modelled without any flexibility present in the system, manifesting what actions are necessary to acquire feasibility. In the second

TABLE 6. Comparing the operation cost of the transmission and distribution grids in a case of congestion in the distribution grid.

Scenario	Distribution grid	Transmission grid
No Flexibility, no voltage regulation	2087.2	123708.5
With Flexibility, no voltage regulation	1392.4	123708
With Flexibility, voltage regulation	1450.8	123707.9

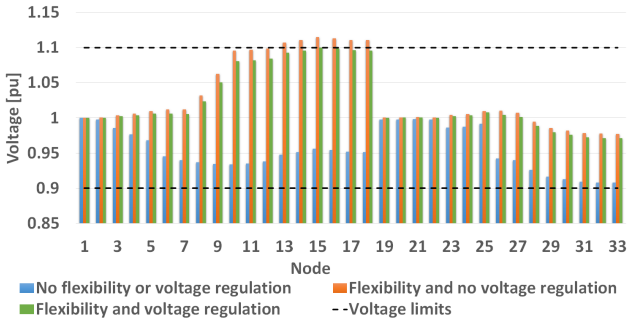

FIGURE 11. Voltage magnitudes for all nodes for all three cases.

case, flexibility is included in the grid to alter the power flows and satisfy the new line constraint. In addition to the flexibility, voltage regulation is also introduced for the third case.

Table 6 shows the comparison of the operation cost in the transmission and distribution grids in the case of congestion in the distribution grid. From Table 6, we can see that the congestion leads to a significant increase in cost for the distribution grid. In the case of voltage regulation, these costs are increasing even more. Flexibility assets are an effective tool for deal with these problems. Therefore, using flexibility assets leads to a reduction of the costs for the distribution grid.

The case starts by analyzing the voltage to determine its magnitudes and the effect flexibility has on it, as shown in Fig. 11.

With no flexibility or voltage regulation presented, low voltage magnitudes can be seen close to the lower bounds for nodes 31, 32, and 33. For this case, where no flexibility is present, load shedding is the only available omodeled acquire feasibility in this grid situation. Due to its high costs, this is a highly inefficient solution and DSO's last resort to handle such an modeled The second case improves these results with the inclusion of flexibility provided by DFR. These improved voltage results are due to the lower voltage drops caused by a more localized production from DFR. Although the new power flow constraint has been satisfied, flexibility has introduced a new issue. During 09:00, nodes 13 to 18 experience overvoltages due to the high production from DFR, leading to voltage violation. In order to counter this issue, case 3 presents a solution where flexibility is also supplemented by voltage regulation. The resulting voltage has a similar profile across the grid compared to case 2, with voltage magnitude on nodes 13 to 18 now below the

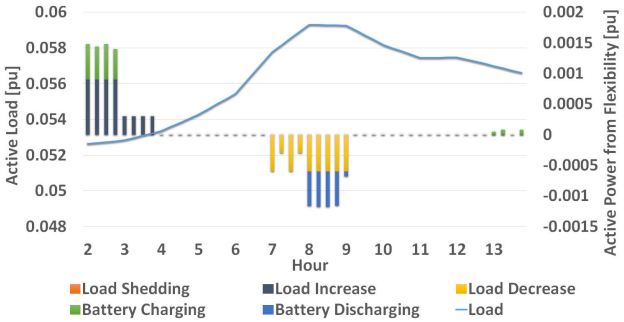

FIGURE 12. Flexibility and load shedding is used to handle the congestion for case 2.

upper voltage bound. The previous issue with low voltages for nodes 31, 32, and 33 is also alleviated, resulting in a far better voltage profile.

Fig. 12 presents the required flexibility dispatch to handle the occurring congestion in the grid. The flexible load has been increased at the simulation start and decreased accordingly during peak load hours when the congestion occurs. The battery has a similar response, where it is charged at the beginning of the simulation and discharged during peak load hours. A short charging period also takes place during the last hour of the simulation. This interval results from the battery's need to end the simulation with the same charge as the initial one. From the model, it is also apparent that no load shedding is required to acquire feasibility, which is a highly desirable outcome [33].

D. SOLVING CONGESTION IN TRANSMISSION GRID

The potential to use flexibility in providing ancillary services is not limited to the distribution grid only [33]. Activating a sufficient amount of DFR can impact the imported power from the transmission grid and alter its flow. With enough capacity, the power flow may also change its direction, feeding power into the transmission grid. Such a case occurs here, where unexpected congestion transpires in the transmission grid after the day-ahead market has already been cleared. This congestion occurs between nodes 7 and 8 of the transmission grid shown in the Fig 5, which limits its transfer capacity to 0.33 pu. Three cases are simulated to showcase the distribution grid's possibilities in supporting the transmission grid. The first case presents the dispatch for a healthy transmission grid, where no congestion has yet occurred. The second case presents the same transmission grid as for case 1, but with congestion of line between nodes 8 and 7. Lastly, in addition to congestion, the last case also includes voltage regulation for all distribution grid nodes.

Table 7 shows the comparison of the operation cost in the transmission and distribution grids in the case of congestion in the transmission grid. From Table 7, we can assume that using flexibility assets leads to a reduction of the costs for both the transmission and distribution grids.

To begin with, voltages for all nodes for operation time 03:30-03:45 are presented in the Fig 13.

TABLE 7. Comparing the operation cost of the transmission and distribution grids in a case of congestion in the transmission grid.

Scenario	Distribution grid	Transmission grid
No Flexibility, no voltage regulation	1356.4	123721.5
With Flexibility, no voltage regulation	1331.3	123718.4
With Flexibility, voltage regulation	1333.5	123719.6

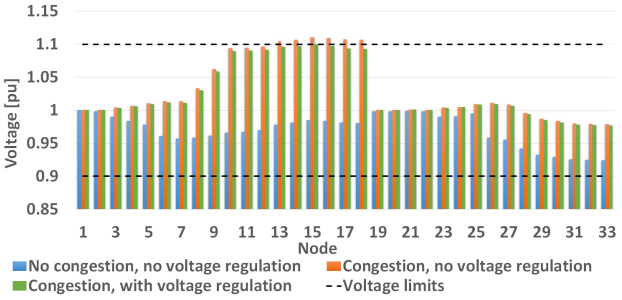

FIGURE 13. Voltage magnitude for all 3 cases for operation time between 03:30 and 03:45.

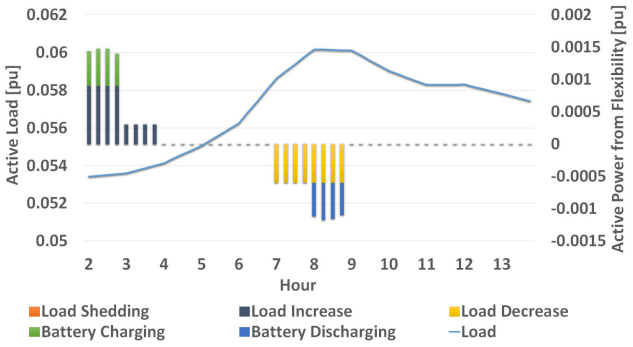

FIGURE 14. Flexibility and load shedding are used in the distribution grid before congestion in the transmission grid has occurred.

From the Fig. 13, case 1 portrays a healthy transmission grid where the voltage magnitudes are within their limits in the distribution grid. For case 2, a significant increase in overall voltages magnitude has occurred. This increase is due to the higher power production in the distribution grid caused by the congestion in the transmission grid. This development has led to over-voltages for nodes 13 to 18 between 03:30 and 03:45. This issue has been alleviated with the inclusion of voltage regulation, resulting in voltage magnitude within boundary limits, as shown by case 3. Fig. 14 presents the total flexibility used for the first case. These results allow the comparison of how the flexibility dispatch has changed due to congestion for cases 2 and 3 in Fig. 15 and Fig 16, respectively.

By comparing Fig. 14 and Fig. 15, a significant change in DFR dispatch has occurred. Due to congestion, a reduction occurs in flexibility provision from the flexible load and batteries, compared to the Fig. 14. In the following Fig. 16, simulation of the same situation with voltage regulation represents DFR dispatch for case 3.

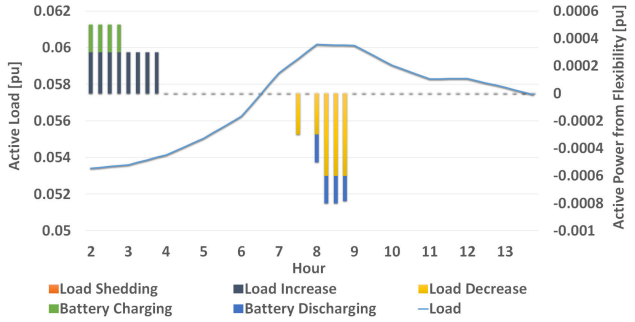

FIGURE 15. Flexibility and load shedding are used in the distribution grid after congestion in the transmission grid has occurred, excluding voltage regulation.

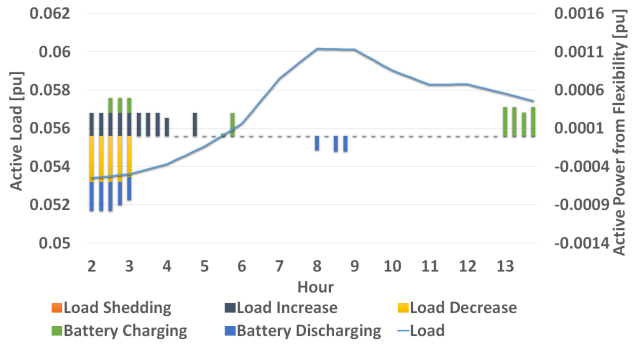

FIGURE 16. Flexibility and load shedding are used in the distribution grid after congestion in the transmission grid has occurred, including voltage regulation.

By including voltage regulation in the distribution grid, flexibility dispatch has been affected by a sizable change, as shown by the Fig. 16. An interesting outcome can be seen in this case, between 02:00 and 03:00. During that period, load shifting has resulted in a contradicting response across the system [33]. To support the transmission system while satisfying voltage constraints, node 10 has increased its consumption, while nodes 5 and 26 have reduced it accordingly. This action is due to the need to reduce the voltages, as shown previously in the Fig. 13. The battery's discharge also occurs during this period before being recharged at the end of the simulation.

The Fig. 17 illustrates the resulting power flow between nodes 7 and 8 as a result of the scheduled power production in the day-ahead market. Here, the green, blue, and yellow lines represent power flow capacity with different measures taken. The black dashed line is the maximum transfer capacity for the line connecting nodes 7 and 8. Case 1 has not taken any measures to meet the congestion requirements, resulting in power flow exceeding the line's transfer capacity, as shown through the blue line. In order to satisfy the transfer capacity in cases 2 and 3, reverse power flow is obtained in the distribution grid by increasing the DFR usage from 02:00 to 06:00. This reverse power flow from the distribution grid results in a power flow reduction between nodes 7 and 8 [33]. The green and yellow lines in the Fig 17 display how the power flow does not exceed the congestion limit in cases 2 and 3.

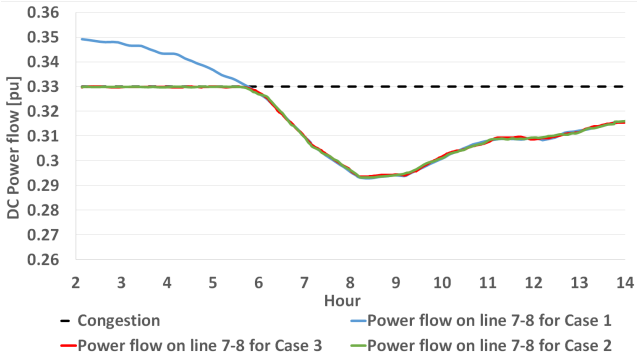

FIGURE 17. The planned power flow for lines 7-8 for case 1, where congestion has not been taken into account.

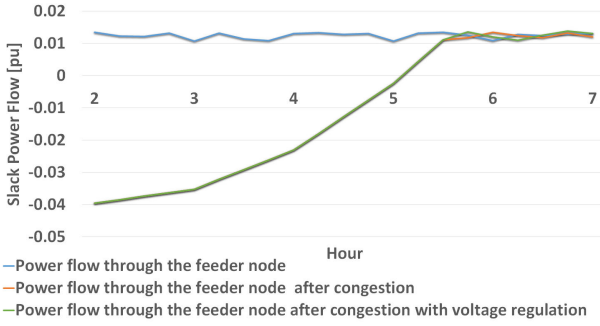

FIGURE 18. Power flow through the slack distribution node.

The Fig. 18 below shows how power flow through the feeder node is effect by the measures taken to counter the congestion in the transmission grid.

For case one in the Fig. 18, a positive flow can be seen, representing a downstream power flow from the transmission to the distribution grid. This flow is also relatively constant throughout the simulation period. This changes when congestion for case 2 occurs, where between 02:00 to 05:00, a negative flow of power emerges. During this period, the active power flows from distribution to the transmission grid. This power flow is necessary to solve the congestion between nodes 7 and 8 of the transmission grid. During these hours, the distribution grid supports the operation of the transmission grid. Case 3 shows a similar result, where the power flow between 02:00 to 05:00 overlaps with case 2. These results also show that the difference in flexibility dispatch between cases 2 and 3 only influences the situation in the distribution grid.

VII. CONCLUSION

The paper explores two main objectives. The first is a theoretical approach regarding FM strategy and design. The second is the development of the multi-period hybrid DC/ACOPF model for seamless TSO-DSO coordination in FM. The considered LFM design presents a solution for improving TSO-TSO/TSO-DSO interaction to unlock, in a cost-effective way, the zero-emission flexibility which is available in assets connected to the transmission and distribution grid. The LFM

strategy also sets criteria for the functionality of the multi-period hybrid AC/DC-OPF model.

The idea behind the multi-period hybrid AC/DC-OPF model was to combine OPF formulations for distribution and transmission grids into one single problem, which unlocks flexibility exchange between these grids. For this purpose, the model applied the SOC-ACOPF for the distribution grid and the DC-OPF method for the transmission grid. These two methods were combined by mathematically formulating the transmission grid and the distribution grid connection constraint. The proposed hybrid AC/DC-OPF model was tested and verified based on widely used network configurations. After this verification, further model expansion took place by including flexibility assets in the distribution grid and the multi-period optimization technique. These measures allowed the development of a multi-period hybrid AC/DC-OPF model capable of simultaneously performing multiple optimal power flow simulations for both the transmission and distribution grid.

In order to demonstrate the applicability of the multi-period hybrid AC/DC-OPF model, test cases with different grid problems were designed. Due to their lower prices, battery and flexible load capacity were the preferred choices for all performed test cases. The flexibility from DG was also used to some extent due to its local placement. Only when grid problems like congestion or voltage problems occurred did DGs increase their power output significantly. This increase in power output is presumably due to the high capacity and location of the DG. When adopting DG to solve voltage or congestion problems, the cost of operation increased significantly. This increase in cost is still a much more preferable and cheaper choice than load shedding.

The test case showed that the potential benefits of using flexibility services are not limited to the distribution grid only. Activating a sufficient amount of flexibility assets can help to solve problems in the transmission grid as well.

Further work that builds upon our investigation will enhance the developed multi-period hybrid AC/DC-OPF model and will focus on the more realistic and complex grid configurations and scenarios of energy use. The proposed Hybrid AC/DC-OPF model in this article is solved as a single optimization problem. In the case of coordination between TSO and several DSOs, in a single optimization problem, the computational complexity will increase significantly. For this reason, as the next step of our investigation, the Hybrid AC/DC-OPF model is extended with the Alternating Direction Method of Multipliers (ADMM). Using the ADMM method allowed us to large-scale problems is decoupled into smaller subproblems for TSOs and DSOs. The Hybrid AC/DC-OPF model for coordination of TSO with multiple DSOs can be solved iteratively by updating Lagrange multipliers according to the ADMM method. In addition, in future work, the reactive power flexibility exchange between TSO and DSO will be considered.

REFERENCES

[1] P. Sorknæs, H. Lund, I. R. Skov, S. Djørup, K. Skytte, P. E. Morthorst, and F. Fausto, "Smart energy markets—Future electricity, gas and heating markets," *Renew. Sustain. Energy Rev.*, vol. 119, Mar. 2020, Art. no. 109655.

[2] M. Maeder, O. Weiss, and K. Boulouchos, "Assessing the need for flexibility technologies in decarbonized power systems: A new model applied to central Europe," *Appl. Energy*, vol. 282, Jan. 2021, Art. no. 116050.

[3] J. J. Alba, C. Vereda, J. Barquín, and E. Moreda, "Market design and regulation to encourage demand aggregation and participation in European energy markets," in *Variable Generation, Flexible Demand*. Amsterdam, The Netherlands: Elsevier, 2021, pp. 393–410.

[4] R. Gutierrez, A. Isabel, E. R. Puente, D. Six, M. Albert, and J. A. Jackson, "D1.2-evaluation of current market architectures and regulatory frameworks and the role of DSOs," EnergyVille, Flemish Res. Inst., KU Leuven, Belgium, Tech. Rep. 608732, 2014.

[5] J. G. de, O. Franz, P. Hermans, and M. Lallemand, "TSO-DSO data management report," TSO-DSO Project Team, CEDEC, entsoe, EDSO Smart Grids, eurelectric, GEODE, Brussels, Belgium, Tech. Rep., 2016.

[6] Z. Yuan and M. R. Hesamzadeh, "Hierarchical coordination of TSO-DSO economic dispatch considering large-scale integration of distributed energy resources," *Appl. Energy*, vol. 195, pp. 600–615, Jun. 2017.

[7] R. D'hulst, J. M. Fernández, E. Rikos, D. Kolodziej, K. Heussen, D. Geibelk, A. Temiz, and C. Caerts, "Voltage and frequency control for future power systems: The ELECTRA IRP proposal," in *Proc. Conf. Voltage Freq. Control Future Power Syst., ELECTRA IRP Proposal*, 2015, pp. 245–250.

[8] A. Ramos, C. De Jonghe, V. Gómez, and R. Belmans, "Realizing the smart grid's potential: Defining local markets for flexibility," *Utilities Policy*, vol. 40, pp. 26–35, Jun. 2016.

[9] S. D. Manshadi and M. E. Khodayar, "A hierarchical electricity market structure for the smart grid paradigm," *IEEE Trans. Smart Grid*, vol. 7, no. 4, pp. 1866–1875, Jul. 2016.

[10] H. Gerard, E. Rivero, and D. Six, "Basic schemes for TSO-DSO coordination and ancillary services provision," SmartNet Deliv D., Eur. Union's Horizon 2020 Res. Innov. Programme, Brussels, Belgium, Tech. Rep. 691405, vol. 1, 2016, p. 12.

[11] S. Bjarghov, M. Loschenbrand, A. U. N. I. Saif, R. A. Pedrero, C. Pfeiffer, S. K. Khadem, M. Rabelhofer, F. Revheim, and H. Farahmand, "Developments and challenges in local electricity markets: A comprehensive review," *IEEE Access*, vol. 9, pp. 58910–58943, 2021.

[12] M. R. AlRashidi and M. E. El-Hawary, "Applications of computational intelligence techniques for solving the revived optimal power flow problem," *Electr. Power Syst. Res.*, vol. 79, no. 4, pp. 694–702, Apr. 2009.

[13] L. Ageeva, M. Majidi, and D. Pozo, "Coordination between TSOs and DSOs: Flexibility domain identification," in *Proc. 12th Medit. Conf. Power Gener., Transmiss., Distrib. Energy Convers. (MEDPOWER)*, 2021, pp. 429–434.

[14] M. Bragin, Y. Dvorkin, and A. Darvishi, "Toward coordinated transmission and distribution operations," in *Proc. IEEE Power Energy Soc. Gen. Meeting (PESGM)*, Aug. 2018, pp. 1–5.

[15] L. F. Ochoa, R. M. Ciric, A. Padilha-Feltrin, and G. P. Harrison, "Evaluation of distribution system losses due to load unbalance," in *Proc. Conf. Eval. Distrib. Syst. Losses Due Load Unbalance*, 2005, pp. 1–4.

[16] J. M. Rupa and S. Ganesh, "Power flow analysis for radial distribution system using backward/forward sweep method," *Int. J. Elect., Comput., Electron., Commun. Eng.*, vol. 8, no. 10, pp. 1540–1554, 2014.

[17] I. Ilieva and B. Bremdal, "Implementing local flexibility markets and the uptake of electric vehicles—The case for Norway," in *Proc. 6th IEEE Int. Energy Conf. (ENERGYCon)*, Gammarth, Tunisia, Sep. 2020, pp. 1047–1052.

[18] D. Van Hertem, J. Verboomen, K. Purchala, R. Belmans, and W. L. Kling, "Usefulness of DC power flow for active power flow analysis with flow controlling devices," in *Proc. Conf. Usefulness DC Power Flow Active Power Flow Anal. With Flow Controlling Devices*, 2006, pp. 58–62.

[19] C. Coffrin and L. Roald, "Convex relaxations in power system optimization: A brief introduction," 2018, *arXiv:1807.07227*.

[20] D. K. Molzahn, "Computing the feasible spaces of optimal power flow problems," *IEEE Trans. Power Syst.*, vol. 32, no. 6, pp. 4752–4763, Nov. 2017.

[21] *Establishing a Guideline on Electricity Balancing OJ L312/6*, Commission Regulation (EU) 2017/2195, Official J. Eur. Union, Eur. Commission, Nov. 2017.

[22] J. P. Chaves, L. Lind, M. Á. Sánchez, Fornié, and L. O. Camacho, "Report of functionalities and services of the Spanish demo," Coordinet, Spain, Tech. Rep. 824414, 2020.
[23] O. K. Olsen, D. Sieraszewski, D. Ivanko, I. Oleinikova, and H. Farahmand, "Hybrid AC/DC optimal power flow modelling approach for coordination in flexibility market," published at the IEEE Conf. SEST 2021.
[24] P. Olivella-Rosell, P. Lloret-Gallego, Í. Munné-Collado, R. Villafafila-Robles, A. Sumper, S. Ø. Ottessen, J. Rajasekharan, and B. A. Bremdal, "Local flexibility market design for aggregators providing multiple flexibility services at distribution network level," *Energies*, vol. 11, no. 4, p. 822, 2018.
[25] Nord Pool. *Trading*. Accessed: Sep. 7, 2022. [Online]. Available: https://www.nordpoolgroup.com/trading/
[26] T. Ackermann, G. Andersson, and L. Söder, "Distributed generation: A definition," *Electr. Power Syst. Res.*, vol. 57, pp. 195–204, Apr. 2001.
[27] *Flexibility in the Energy Transition: A Toolbox for Electricity DSOs*, C. EDSO and G. Eurelectric, 2018.
[28] J. Sun and L. Tesfatsion, "DC optimal power flow formulation and solution using QuadProgJ," Iowa State Univ., Ames, IA, USA, Econ. Work. Papers 2002-2016, 2010, p. 253.
[29] W. E. Hart, C. Laird, J.-P. Watson, and D. L. Woodruff, *Pyomo-Optimization Modeling in Python*. USA: Springer, 2017.
[30] M. E. Baran and F. F. Wu, "Network reconfiguration in distribution systems for loss reduction and load balancing," *IEEE Power Eng. Rev.*, vol. 9, no. 4, pp. 101–102, 1989.
[31] P. M. Anderson and A. A. Fouad, *Power System Control and Stability*. Hoboken, NJ, USA: Hoboken, NJ, USA: Wiley, 2008.
[32] M. Henryk and K. Antony, *Voltage Characteristics in Public Distribution System*, Standard EN 50160, Wroclaw Univ. Technol., Wrocław, Poland, 2004.
[33] O. K. Olsen and D. Sieraszewski, *Model Development for DSO-TSO Coordination in a Local Flexibility Market*, document, NTNU, Trondheim, Norway, 2021.
[34] G. Papazoglou and P. Biskas, "Review of methodologies for the assessment of feasible operating regions at the TSO–DSO interface," *Energies*, vol. 15, no. 14, p. 5147, Jul. 2022.
[35] S. Riaz and P. Mancarella, "Modelling and characterisation of flexibility from distributed energy resources," *IEEE Trans. Power Syst.*, vol. 37, no. 1, pp. 38–50, Jan. 2022.
[36] D. A. Contreras and K. Rudion, "Time-based aggregation of flexibility at the TSO-DSO interconnection point," in *Proc. IEEE Power Energy Soc. Gen. Meeting (PESGM)*, Aug. 2019, pp. 1–5.

DAMIAN SIERASZEWSKI received the bachelor's degree in electrical engineering from the Arctic University of Norway, and the master's degree from the Norwegian University of Science and Technology. Currently, he is an Engineer in electrical safety and operation with Equinor Hammerfest, Troms og Finnmark, Norway. His research interests include electrical operation, optimization modeling, electrical engineering, TSO-DSO coordination, and flexibility markets modeling.

OLE KJÆRLAND OLSEN received the bachelor's degree in electrical engineering from the Arctic University of Norway and the master's degree from the Norwegian University of Science and Technology (NTNU). He is currently a Production Engineer with Sira-Kvina Power Company, Rogaland, Norway. His research interests include production planning and operation, financial settlement, optimization modeling, electrical engineering, TSO-DSO coordination, and flexibility markets modeling.

DMYTRO IVANKO received the Ph.D. degree (technical sciences) from the Electric Power Supply Department, National Technical University, Ukraine Igor Sikorsky Kyiv Polytechnic Institute, Kiev, Ukraine, in 2017, and the Ph.D. degree from the Energy and Process Engineering Department, Norwegian University of Science and Technology (NTNU), Trondheim, Norway, in 2021. He is currently a Postdoctoral Researcher with the Department of Electric Power Engineering, NTNU. His research interests include flexibility market, energy management, TSO-DSO coordination, the analysis of energy use, the monitoring of energy efficiency, data mining for energy monitoring, machine learning, and the data-driven analysis of energy use.

IRINA OLEINIKOVA received the Ph.D. degree in power engineering from Riga Technical University. She is currently a Professor with the Department of Electric Power Engineering, and the Head of the Power System Operation and Analysis Research Group. She is also the NTNU Smart Grid Team Leader. She is also a Steering Committee Member of the European Energy Research Alliance Joint Program on Smart Grids and an Expert in ISGAN Annex 6. Her research interests include power system operation and planning, smart grids and the electricity market, with more than ten years of management experience to carry out research projects independently with the new scientific tasks developments and application in field of smart grids, playing an active role in exploring research materials for industrial sector in Nordic and Baltic Countries.

HOSSEIN FARAHMAND (Senior Member, IEEE) received the Ph.D. degree from the Department of Electric Power Engineering, Norwegian University of Science and Technology (NTNU), Trondheim, Norway, in 2012. From 2012 to 2015, he was a Research Scientist with the Department of Energy Systems, SINTEF Energy Research, Trondheim. He is currently an Associate Professor with the Department of Electric Power Engineering, NTNU. His research interests include power system balancing, power market analysis, demand-side management, and flexibility operation in distribution systems. He has been involved in several EU-projects, including INVADE H2020, EU FP7 TWENTIES, EU FP7 eHighway2050, and IRPWIND. He serves as an Associate Editor for IEEE TRANSACTIONS ON ENERGY MARKETS, POLICY AND REGULATION.